

Research



Cite this article: Saha J, Kumar J, Heinrich S. 2018 On the approximate solutions of fragmentation equations. *Proc. R. Soc. A* **474**: 20170541.
<http://dx.doi.org/10.1098/rspa.2017.0541>

Received: 4 August 2017

Accepted: 18 December 2017

Subject Areas:

computer modelling and simulation, chemical engineering, computational mathematics

Keywords:

population balance equations, fragmentation, finite volume scheme, volume conservation, convergence

Author for correspondence:

Jitraj Saha

e-mail: jitraj@iitkgp.ac.in

¹Department of Mathematics, Indian Institute of Technology Kharagpur, Kharagpur 721302, India

²Institute of Solids Process Engineering and Particle Technology, Hamburg University of Technology, Hamburg 21073, Germany

JS, 0000-0002-8864-5537

A numerical model based on the finite volume scheme is proposed to approximate the binary breakage problems. Initially, it is considered that the particle fragments are characterized by a single property, i.e. particle's volume. We then investigate the extension of the proposed model for solving breakage problems considering two properties of particles. The efficiency to estimate the different moments with good accuracy and simple extension for multi-variable problems are the key features of the proposed method. Moreover, the mathematical convergence analysis is performed for one-dimensional problems. All mathematical findings and numerical results are validated over several test problems. For numerical validation, we propose the extension of Bourgade & Filbet (2008 *Math. Comput.* **77**, 851–882. (doi:10.1090/S0025-5718-07-02054-6)) model for solving two-dimensional pure breakage problems. In this aspect, numerical treatment of the two-dimensional binary breakage models using finite volume methods can be treated to be the first instance in the literature.

1. Introduction

Events of particle fragmentation (or breakage) occur in several industrial sectors such as chemical engineering [1–4], food processing [5–7], pharmaceutical [8–10], comminution in mineral processing [11–14], etc., and, in different natural and astrophysical phenomena [15–17]. Therefore, theoretical researchers have gained interest to discuss on different model equations involving particle breakage [18–22].

The mathematical equations representing different particulate processes are well known in the literature as the population balance equations (PBEs). Here, we

consider the following mathematical model representing particle fragmentation in one dimension [23];

$$\frac{\partial n(x, t)}{\partial t} = 2 \int_x^\infty F(x, y - x)n(y, t) dy - n(x, t) \int_0^x F(x - y, y) dy, \quad (1.1)$$

along with the initial data

$$n(x, 0) = n_0(x) \geq 0, \quad \text{for all } x > 0. \quad (1.2)$$

In equation (1.1), $n(x, t)(\geq 0)$ denotes the number density of particles of volume $x(>0)$ at time $t(\geq 0)$. The fragmentation kernel $F(x, y)$ represents particle breakage rate of volume $(x + y)$ into x and y . In general, it is considered that F is a non-negative, symmetric function of x and y . The first integral on the right-hand side of (1.1) is called the *birth* term, as it represents the inclusion of particles of volume x in the system due to the breakage of bigger particles. On the other hand, the second integral corresponds to the removal (or exclusion) of particles of volume x due to its breakage into smaller fragments $(x - y)$ and y . Therefore, it is referred as the *death* term. As F is symmetric, either of the resulting fragments in the birth term can form a particle of volume x . Therefore, the factor 2 is introduced to account those particle formations. Without loss of generality, all the concerned quantities in equation (1.1) are considered in dimensionless form [24].

In general, different integral properties of the density function play important roles for the PBEs, as some of them correspond to the physical properties such as total number and volume. Therefore, efficient estimation of these moments is required while approximating the PBEs. In this regard, the p th moment of the density function is defined as

$$M_p(t) = \int_0^\infty x^p n(x, t) dx \quad p = 1, 2, \dots \quad (1.3)$$

In particular, the zeroth and the first moments are respectively proportional to the total number and total volume of the particles present in the system. From (1.1) and (1.3), by simple change in the order of integrations, it can be obtained that

$$\frac{dM_p(t)}{dt} = \int_0^\infty n(x, t) \int_0^x [2y^p - x^p] F(x - y, y) dy dx, \quad (1.4)$$

when all the integrals exist finitely [23]. Therefore for $p = 1$, using the symmetric nature of F , we obtain

$$\frac{dM_1(t)}{dt} = 0. \quad (1.5)$$

Hence, a system is said to obey the *volume conservation laws* if it satisfies the relation (1.5). Furthermore, the temporal change of the zeroth moment ($p = 0$) is obtained as follows:

$$\frac{dM_0(t)}{dt} = \int_0^\infty n(x, t) \int_0^x F(x - y, y) dy dx. \quad (1.6)$$

However, equation (1.6) can be written in a closed form of higher moments for some suitable choice of $F(x, y)$. Thus from the physical aspect, an efficient numerical model approximating the PBEs is expected to predict the total volume and the total number of the particles in the system with good accuracy. This notion when expressed mathematically, we say that an efficient scheme should obey relations (1.5) and (1.6).

Another form of the PBEs, known as the *volume conservative* formulation, is widely available in the literature [25,26]. In particular, the conservative formulation of breakage equations reads as

$$\frac{x \partial n(x, t)}{\partial t} = \frac{\partial}{\partial x} \left[\int_0^x \int_{x-u}^\infty u F(u, v) n(u + v) dv du \right]. \quad (1.7)$$

Using Leibniz's rule for differentiation under the integral sign and symmetric behaviour of F , we can easily show that relations (1.7) and (1.1) are equivalent mathematical expressions. However, (1.7) has gained importance because the schemes originated from it possess the natural feature to obey volume conservation laws (1.5).

In several industrial sectors such as comminution in mineral processing industries and chemical plants, the multi-dimensional fragmentation models are used considerably [12,27,28]. Here, multi-dimensional fragmentation problems indicate that the particle fragments are described by more than one internal variables. In this regard, several authors have discussed upon the physical aspect of the solutions and their different moments for the multi-dimensional problems [29–32]. A rigorous study on the phase transition states that under certain kinetic rate, particles of nearly zero volume are produced, thus leading to the break down of the conservative nature of the system. However, in several industrial applications, like during the separation of minerals from their ores, the break down of conservative nature cannot be entertained as it increases the process cost considerably. In this article, we concentrate our study towards the kinetic kernels which obeys the conservative nature of the physical system, and aim to develop a robust numerical scheme which approximates different physical properties of the system efficiently.

Many numerical schemes dealing with the discretization of (1.1) or (1.7) have been proposed in recent years, and it would not be possible to give an exhaustive list. In this regard, the sectional methods in [33–35], moment methods in [36,37], finite-element methods in [38–40], finite volume methods in [25,26,41–44] have gathered interest of the researchers. In particular, approximations based on finite volume methods have gained importance as they possess simple extension for solving higher dimensional problems [42,45]. There are several evidences in the literature where the development of finite volume schemes approximating pure aggregation problems [25,42,45–49] has been discussed. However, the approximation of multi-dimensional breakage problems using finite volume methods has not been discussed in the literature. Our intention is to obtain a numerical model for solving both one- and two-dimensional breakage problems.

In this paper, we propose a finite volume scheme for solving one-dimensional fragmentation equations and extend it for the two-dimensional problems. The new model is derived from the classical equation given by (1.1). Therefore, it has simple mathematical formulation and is robust to apply on both uniform and non-uniform grids. A detailed convergence analysis of the one-dimensional scheme is also performed. To compare the efficiency of our proposed model, we consider the standard one-dimensional scheme of [26] as our reference model. Because the scheme in [26] does not possess its multi-dimensional extension for solving fragmentation problems, we introduce its two-dimensional extension in order to validate our proposed scheme numerically.

The article is organized as follows. Section 2, contains the derivation of the discrete models. In §3, we discuss the mathematical convergence analysis of the one-dimensional model. Extension of [26] model in two dimensions along with the numerical verification of the proposed model is given in §4.

2. New formulations

(a) One-dimensional model

The volume variable x in equation (1.1) ranges over $(0, \infty)$. In order to apply a numerical method, we need to fix a finite range of the computational domain. Let for some finite $R(> 0)$, all the particles having volume range $(0, R]$ take part in the kinetic interactions. Also, consider $0 \leq t \leq T < \infty$. Hence, the truncated equation (1.1) reads as

$$\frac{\partial n(x, t)}{\partial t} = 2 \int_x^R F(x, y - x) n(y, t) dy - n(x, t) \int_0^x F(x - y, y) dy, \quad (2.1)$$

along with the initial data

$$n(x, 0) = n_0(x) \geq 0, \quad x \in (0, R].$$

Let $(0, R] =: D$ is discretized into $I (< \infty)$ sub-intervals A_i , where

$$A_i := (x_{i-1/2}, x_{i+1/2}], \quad i = 1, 2, \dots, I$$

with $x_{1/2} = 0$, $x_{I+1/2} = R$ and $\Delta x_i := x_{i+1/2} - x_{i-1/2}$. Let the mid-point of each Λ_i , i.e. $x_i := (x_{i+1/2} + x_{i-1/2})/2$, represents the particle size of that cell and we call it *pivot* or *grid point* of the cell. Furthermore, let $\Delta x := \max_i \Delta x_i$, $\delta x := \min_i \Delta x_i$ and there exists a constant \mathcal{K} such that

$$\frac{\Delta x}{\delta x} \leq \mathcal{K}. \quad (2.2)$$

Let $N_i(t)$ denote the number of particles in the i th cell, i.e.

$$N_i(t) := \int_{x_{i-1/2}}^{x_{i+1/2}} n(x, t) dx.$$

For notational convenience, we simply drop the argument t from $N_i(t)$ and write it as N_i . In this regard, it should not be mistaken that N_i is independent of t . Therefore, integrating (2.1) over each Λ_i , we obtain the following system of equations:

$$\frac{dN_i}{dt} = B_i - D_i, \quad i = 1, 2, \dots, I,$$

with the initial data,

$$N_i^n = N_i(0) = \int_{x_{i-1/2}}^{x_{i+1/2}} n_0(x) dx$$

and

$$B_i := 2 \int_{x_{i-1/2}}^{x_{i+1/2}} \int_x^R F(x, y-x)n(y, t) dy dx, \quad D_i := \int_{x_{i-1/2}}^{x_{i+1/2}} n(x, t) \int_0^x F(x-y, y) dy dx.$$

Changing the order of integration, B_i is written as

$$\begin{aligned} B_i &= 2 \int_{x_{i-1/2}}^{x_{i+1/2}} \int_{x_{i-1/2}}^y F(x, y-x)n(y, t) dx dy + 2 \int_{x_{i+1/2}}^R \int_{x_{i-1/2}}^{x_{i+1/2}} F(x, y-x)n(y, t) dx dy \\ &= 2 \int_{x_{i-1/2}}^{x_{i+1/2}} \int_{x_{i-1/2}}^y F(x, y-x)n(y, t) dx dy + 2 \sum_{k=i+1}^I \int_{x_{k-1/2}}^{x_{k+1/2}} \int_{x_{i-1/2}}^{x_{i+1/2}} F(x, y-x)n(y, t) dx dy. \end{aligned}$$

Applying quadrature formulae to the outer integrals, the right-hand side of B_i reads as

$$\begin{aligned} B_i &= 2N_i \int_{x_{i-1/2}}^{x_i} F(x_i-x, x) dx + 2 \sum_{k=i+1}^I N_k \int_{x_{i-1/2}}^{x_{i+1/2}} F(x_k-x, x) dx + \mathcal{O}(\Delta x^3) \\ &= 2 \sum_{k=i}^I N_k \int_{x_{i-1/2}}^{p_k^i} F(x_k-x, x) dx + \mathcal{O}(\Delta x^3). \end{aligned} \quad (2.3)$$

Here, we denote

$$p_k^i := \begin{cases} x_i, & \text{when } k = i, \\ x_{i+1/2}, & \text{otherwise.} \end{cases}$$

Similarly, applying quadrature formula to the outer integrals of D_i , we obtain

$$D_i = N_i \int_0^{x_i} F(x_i-y, y) dy + \mathcal{O}(\Delta x^3). \quad (2.4)$$

Our aim is to obtain a numerical scheme which obeys volume-conservative laws and, predicts the total particle number with good accuracy. Therefore, we propose the following numerical scheme

to serve the purpose.

$$\frac{d\hat{N}_i}{dt} = 2 \sum_{k=i}^I \omega_k^b \hat{N}_k \int_{x_{i-1/2}}^{p_i^k} F(x_k - x, x) dx - \omega_i^d \hat{N}_i \int_0^{x_i} F(x_i - x, x) dx, \quad (2.5)$$

where \hat{N}_i is the numerical approximation of N_i and ω_k^b, ω_i^d are the weight functions given by

$$\omega_k^b := \frac{\int_0^{x_k} xF(x_k - x, x) dx}{\sum_{j=1}^k \int_{x_{j-1/2}}^{p_j^k} (2x - x_j)F(x_k - x, x) dx} \quad (2.6)$$

and

$$\omega_i^d := \frac{\omega_i^b \sum_{j=1}^i x_j \int_{x_{j-1/2}}^{p_j^i} F(x_i - x, x) dx}{\int_0^{x_i} xF(x_i - x, x) dx} \quad (2.7)$$

for all $k, i = 2, 3, \dots, I$ along with $\omega_1^b = \omega_1^d = 1$.

It is to be noted that the weight functions ω_k^b, ω_k^d are the key features of the proposed model (2.5), as they play an important role to control the accuracy of the desired moments. We now proceed to verify our claim by evaluating the discrete first and zeroth moments obtained from the scheme (2.5). Let us multiply both sides of (2.5) by x_i and take sum over i to obtain

$$\frac{d}{dt} \sum_{i=1}^I x_i \hat{N}_i = \sum_{k=1}^I \hat{N}_k \left[2\omega_k^b \sum_{i=1}^k x_i \int_{x_{i-1/2}}^{p_i^k} F(x_k - x, x) dx - \omega_k^d x_k \int_0^{x_k} F(x_k - x, x) dx \right].$$

Recalling the weight ω_k^b (2.6) and using the following relation:

$$x_k \int_0^{x_k} F(x_k - x, x) dx = 2 \int_0^{x_k} xF(x_k - x, x) dx \quad (2.8)$$

from [50], we obtain

$$\frac{d}{dt} \sum_{i=1}^I x_i \hat{N}_i = 2 \sum_{k=1}^I \hat{N}_k \omega_k^b \left[\sum_{i=1}^k x_i \int_{x_{i-1/2}}^{p_i^k} F(x_k - x, x) dx - \sum_{i=1}^k x_i \int_{x_{i-1/2}}^{p_i^k} F(x_k - x, x) dx \right] = 0,$$

for all \hat{N}_i and F . Thus, system (2.5) obeys volume conservation laws.

Now taking sum over i on both sides of (2.5), the discrete zeroth moment is written as

$$\frac{d}{dt} \sum_{i=1}^I \hat{N}_i = \sum_{k=1}^I \hat{N}_k [2\omega_k^b - \omega_k^d] \int_0^{x_k} F(x_k - x, x) dx.$$

Recalling the weights ω_k^b and ω_k^d , the factor $(2\omega_k^b - \omega_k^d)$ is simplified into

$$\begin{aligned} 2\omega_k^b - \omega_k^d &= \frac{\omega_k^b}{\int_0^{x_k} xF(x_k - x, x) dx} \left[2 \int_0^{x_k} xF(x_k - x, x) dx - \sum_{j=1}^k x_j \int_{x_{j-1/2}}^{p_j^k} F(x_k - x, x) dx \right] \\ &= \frac{1}{\sum_{j=1}^k \int_{x_{j-1/2}}^{p_j^k} (2x - x_j)F(x_k - x, x) dx} \sum_{j=1}^k \int_{x_{j-1/2}}^{p_j^k} (2x - x_j)F(x_k - x, x) dx = 1. \end{aligned}$$

Hence, we obtain

$$\frac{d}{dt} \sum_{i=1}^I \hat{N}_i = \sum_{i=1}^I \hat{N}_i \int_0^{x_i} F(x_i - x, x) dx.$$

It is to be noted that the right-hand side of the above relation is analogous to its continuous counterpart given in (1.6). Therefore, the scheme (2.5) is expected to predict the zeroth moment with high accuracy. This claim is validated in §4 over some test problems.

(b) Two-dimensional model

We now introduce the finite volume approximation of the fragmentation problems by considering two internal variables in the distribution function. Basically, we will introduce the two-dimensional extension of the new scheme (2.5), which conserves the total volume and predicts the particle number with high accuracy.

Let $n(x, y, t)$ be the number density of particles having properties x, y at time $t(\geq 0)$. Also let $F(x, y | x', y')(\geq 0)$ denote the kinetic rate at which particles with properties (x, y) and (x', y') are produced during the breakage event of larger particles with properties $(x' + x)$ and $(y' + y)$. Referring to equation (1.1), the two-dimensional form of classical breakage equation (1.1) is written as

$$\begin{aligned} \frac{\partial n(x, y, t)}{\partial t} = & 2 \int_x^\infty \int_y^\infty F(x' - x, y' - y | x, y) n(x', y', t) dy' dx' \\ & - n(x, y, t) \int_0^x \int_0^y F(x - x', y - y' | x', y') dy' dx', \end{aligned} \quad (2.9)$$

along with initial condition

$$n(x, y, 0) = n_0(x, y) \geq 0 \quad \text{for all } x, y > 0.$$

Furthermore, the moments of the density function $n(x, y, t)$ are given by

$$M_{i,j}(t) = \int_0^\infty \int_0^\infty x^i y^j n(x, y, t) dy dx \quad i, j = 1, 2, \dots$$

Like the one-dimensional problem, the zeroth moment $M_{0,0}(t)$ corresponds to the total number of particles and, the temporal change of zeroth moment can be obtained as

$$\frac{dM_{0,0}(t)}{dt} = \int_0^\infty \int_0^\infty n(x, y, t) \int_0^x \int_0^y F(x - x', y - y' | x', y') dy' dx'. \quad (2.10)$$

However, in this case, there exists two first-order moments $M_{1,0}(t)$ and $M_{0,1}(t)$. Here, $M_{1,0}(t)$ corresponds to the total volume of particles with property x . Similar explanation holds for $M_{0,1}(t)$. Thus, for a volume-conservative system, we should have

$$\frac{d}{dt} [M_{1,0}(t) + M_{0,1}(t)] = 0. \quad (2.11)$$

Let us consider, $0 < x \leq R_x < \infty$, $0 < y \leq R_y < \infty$ and $0 \leq t \leq T$. Therefore, the truncated form of equation (2.9) is written as

$$\begin{aligned} \frac{\partial n(x, y, t)}{\partial t} = & 2 \int_x^{R_x} \int_y^{R_y} F(x' - x, y' - y | x, y) n(x', y', t) dy' dx' \\ & - n(x, y, t) \int_0^x \int_0^y F(x - x', y - y' | x', y') dy' dx'. \end{aligned}$$

Let I and J be any positive integer. We now discretize the truncated domain $(0, R_x] \times (0, R_y]$ in finite number of rectangular cells $C_{i,j} := (x_{i-1/2}, x_{i+1/2}] \times (y_{j-1/2}, y_{j+1/2}]$, where $1 \leq i \leq I$, $1 \leq j \leq J$ with $x_{1/2} = y_{1/2} = 0$, $x_{I+1/2} = R_x$ and $y_{J+1/2} = R_y$. The centre of each cell $C_{i,j}$, that is, (x_i, y_j) is considered to be the pivot. Let $\hat{n}_{i,j}$ be the numerical approximation of the average density function in the rectangle $C_{i,j}$ and we denote $\hat{N}_{i,j} := \hat{n}_{i,j} \Delta x_i \Delta y_j$. Proceeding in a similar manner as done for the one-dimensional problem, we write the two-dimensional extension of the proposed model (2.5) as

$$\begin{aligned} \frac{d\hat{N}_{i,j}}{dt} = & 2 \sum_{k=i}^I \sum_{l=j}^J \omega_{k,l}^b \hat{N}_{k,l} \int_{x_{i-1/2}}^{x_k} \int_{y_{j-1/2}}^{y_l} F(x_k - x, y_l - y | x, y) dy dx \\ & - \omega_{i,j}^d \hat{N}_{i,j} \int_0^{x_i} \int_0^{y_j} F(x_i - x, y_j - y | x, y) dy dx. \end{aligned} \quad (2.12)$$

Here, the weight functions are given by

$$\omega_{k,l}^b := \frac{\int_0^{x_k} \int_0^{y_l} (x+y)F(x_k-x, y_l-y | x, y) dy dx}{\sum_{i=1}^k \sum_{j=1}^l \int_{x_{i-1/2}}^{p_i^k} \int_{y_{j-1/2}}^{q_j^l} (2x+2y-x_i-y_j)F(x_k-x, y_l-y | x, y) dy dx} \quad (2.13)$$

and

$$\omega_{k,l}^d := \frac{\omega_{k,l}^b \sum_{i=1}^k \sum_{j=1}^l (x_i+y_j) \int_{x_{i-1/2}}^{p_i^k} \int_{y_{j-1/2}}^{q_j^l} F(x_k-x, y_l-y | x, y) dy dx}{\int_0^{x_k} \int_0^{y_l} (x+y)F(x_k-x, y_l-y | x, y) dy dx} \quad (2.14)$$

for all $k=1, 2, \dots, I, l=1, 2, \dots, J$ with $\omega_{1,1}^b = \omega_{1,1}^d = 1$. In the above relations, we denote

$$q_l^j := \begin{cases} y_j, & \text{when } l=j, \\ y_{j+1/2}, & \text{otherwise.} \end{cases}$$

Proposition 2.1. *The numerical scheme (2.12) obeys volume conservation laws and, the zeroth numerical moment follows the discrete analogy of relation (2.10).*

Proof. We first calculate the time derivative of the sum of first-order discrete moments. Therefore, multiplying both sides of (2.12) with (x_i+y_j) and taking sum over i and j , we can write

$$\begin{aligned} \frac{d}{dt} \sum_{i=1}^I \sum_{j=1}^J (x_i+y_j) \hat{N}_{i,j} &= 2 \sum_{k=1}^I \sum_{l=1}^J \omega_{k,l}^b \hat{N}_{k,l} \sum_{i=1}^k \sum_{j=1}^l (x_i+y_j) \int_{x_{i-1/2}}^{p_i^k} \int_{y_{j-1/2}}^{q_j^l} F(x_k-x, y_l-y | x, y) dy dx \\ &\quad - \sum_{k=1}^I \sum_{l=1}^J \omega_{k,l}^d \hat{N}_{k,l} (x_k+y_l) \int_0^{x_k} \int_0^{y_l} F(x_k-x, y_l-y | x, y) dy dx. \end{aligned}$$

Substituting $\omega_{k,l}^d$ and using the relation

$$(x_k+y_l) \int_0^{x_k} \int_0^{y_l} F(x_k-x, y_l-y | x, y) dy dx = 2 \int_0^{x_k} \int_0^{y_l} (x+y)F(x_k-x, y_l-y | x, y) dy dx,$$

to the second term in the right-hand side, we obtain

$$\begin{aligned} \frac{d}{dt} \sum_{i=1}^I \sum_{j=1}^J (x_i+y_j) \hat{N}_{i,j} &= \sum_{k=1}^I \sum_{l=1}^J 2\omega_{k,l}^b \hat{N}_{k,l} \sum_{i=1}^k \sum_{j=1}^l (x_i+y_j) \int_{x_{i-1/2}}^{p_i^k} \int_{y_{j-1/2}}^{q_j^l} F(x_k-x, y_l-y | x, y) dy dx \\ &\quad - \sum_{k=1}^I \sum_{l=1}^J 2\omega_{k,l}^b \hat{N}_{k,l} \sum_{i=1}^k \sum_{j=1}^l (x_i+y_j) \int_{x_{i-1/2}}^{p_i^k} \int_{y_{j-1/2}}^{q_j^l} F(x_k-x, y_l-y | x, y) dy dx \\ &= 0, \end{aligned}$$

for all $\hat{N}_{k,l}$ and F . Therefore, system (2.12) obeys volume conservation laws.

Next, we calculate the temporal change of discrete zeroth moment. Therefore,

$$\begin{aligned} \frac{d}{dt} \sum_{i=1}^I \sum_{j=1}^J \hat{N}_{i,j} &= \sum_{i=1}^I \sum_{j=1}^J \sum_{k=i}^I \sum_{l=j}^J 2\omega_{k,l}^b \hat{N}_{k,l} \int_{x_{i-1/2}}^{p_i^k} \int_{y_{j-1/2}}^{q_j^l} F(x_k-x, y_l-y | x, y) dy dx \\ &\quad - \sum_{i=1}^I \sum_{j=1}^J \omega_{i,j}^d \hat{N}_{i,j} \int_0^{x_i} \int_0^{y_j} F(x_i-x, y_j-y | x, y) dy dx. \end{aligned}$$

Proceeding in a manner similar to the previous one and using the weight functions given in (2.12), we shall obtain

$$\frac{d}{dt} \sum_{i=1}^I \sum_{j=1}^J \hat{N}_{ij} = \sum_{i=1}^I \sum_{j=1}^J \hat{N}_{ij} \int_0^{x_i} \int_0^{y_j} F(x_i - x, x | y_j - y, y) dy dx.$$

Thus, our claim is justified. ■

3. Convergence analysis for one-dimensional model

In this part of our study, we prove that when the fragmentation kernel F satisfies certain regularity conditions over a closed interval, the proposed one-dimensional scheme (2.5) exhibits a second-order convergence rate, irrespective of the meshes used in discretization.

Let us denote

$$\hat{B}_i := 2 \sum_{k=i}^I \omega_k^b \hat{N}_k \int_{x_{i-1/2}}^{p_k^i} F(x_k - x, x) dx \quad (3.1)$$

and

$$\hat{D}_i := \omega_i^d \hat{N}_i \int_0^{x_k} F(x_i - x, x) dx. \quad (3.2)$$

Therefore, the one-dimensional semi-discrete model is written as

$$\frac{d\hat{N}_i}{dt} = \hat{B}_i - \hat{D}_i, \quad i = 1, 2, \dots, I,$$

with the initial condition

$$\hat{N}_i(0) = N_i(0).$$

Let $\hat{\mathbf{N}} = [\hat{N}_1, \hat{N}_2, \dots, \hat{N}_I]^T$ denote the numerical solutions in vector form. Therefore, the above formulations take the following spatially discretized vector form in \mathbb{R}^I

$$\left. \begin{aligned} \frac{d\hat{\mathbf{N}}}{dt} &= \hat{\mathbf{B}}(\hat{\mathbf{N}}) - \hat{\mathbf{D}}(\hat{\mathbf{N}}) =: \hat{\mathbf{J}}(\hat{\mathbf{N}}) \\ \hat{\mathbf{N}}(0) &= \mathbf{N}^{\text{in}} \end{aligned} \right\} \quad (3.3)$$

where $\hat{\mathbf{B}}, \hat{\mathbf{D}} \in \mathbb{R}^I$ are the functions of $\hat{\mathbf{N}}$ whose i th components are $\hat{B}_i(\hat{\mathbf{N}})$ and $\hat{D}_i(\hat{\mathbf{N}})$, respectively and $\hat{\mathbf{J}}(\hat{\mathbf{N}}) = [J_1(\hat{N}_1), J_2(\hat{N}_2), \dots, J_I(\hat{N}_I)]$.

In this part of our study, we shall use definitions 3.1–3.3 and theorems 3.1–3.2 listed in [50] to establish the proposed results. Let the discrete L^1 norm on \mathbb{R}^I be defined as

$$\|\mathbf{N}(t)\| = \sum_{i=1}^I |N_i(t)|. \quad (3.4)$$

Let $\hat{\mathbf{J}}(\mathbf{N})$ be the vector function obtained by replacing the numerical solution $\hat{\mathbf{N}}$ with the true solution $\mathbf{N} := [N_1, N_2, \dots, N_I]^T$.

We now proceed to establish the stability of our proposed one-dimensional scheme (2.5) by examining the Lipschitz condition.

Proposition 3.1. Consider that $F(x, y) \in C^2([0, R] \times [0, R])$. Then $\hat{\mathbf{J}}(\mathbf{N})$ satisfies Lipschitz condition for all $\mathbf{N}, \hat{\mathbf{N}} \in \mathbb{R}^I$, with the Lipschitz constant being independent of Δx .

Proof. We calculate the norm $\|\mathbf{J}(\mathbf{N}) - \mathbf{J}(\hat{\mathbf{N}})\|$.

$$\begin{aligned} \|\mathbf{J}(\mathbf{N}) - \mathbf{J}(\hat{\mathbf{N}})\| &= \sum_{i=1}^I |J_i(N_i) - J_i(\hat{N}_i)| \leq 2 \sum_{i=1}^I \sum_{k=i}^I \omega_k^b \int_{x_{i-1/2}}^{p_i^k} F(x_k - x, x) dx |N_k - \hat{N}_k| \\ &\quad + \sum_{i=1}^I \omega_i^d \int_0^{x_i} F(x_i - x, x) dx |N_i - \hat{N}_i|. \end{aligned}$$

It is considered that $\omega_1^b = \omega_1^d = 0$. Therefore, changing the order of the summation of the first term, the above relation is re-written as

$$\begin{aligned} \|\mathbf{J}(\mathbf{N}) - \mathbf{J}(\hat{\mathbf{N}})\| &= 2 \underbrace{\sum_{k=2}^I \omega_k^b |N_k - \hat{N}_k| \sum_{i=1}^k \int_{x_{i-1/2}}^{p_i^k} F(x_k - x, x) dx}_{=:T_1} \\ &\quad + \underbrace{\sum_{k=2}^I \omega_k^d \int_0^{x_k} F(x_k - x, x) dx |N_k - \hat{N}_k|}_{=:T_2}. \end{aligned}$$

Let us first consider the term T_1 . Recalling the weight ω_k^b (2.6), we obtain

$$\omega_k^b = \frac{\int_0^{x_k} x F(x_k - x, x) dx}{\sum_{i=1}^k \int_{x_{i-1/2}}^{p_i^k} (2x - x_i) F(x_k - x, x) dx} = 1 + \frac{\sum_{i=1}^k \int_{x_{i-1/2}}^{p_i^k} (x_i - x) F(x_k - x, x) dx}{\sum_{i=1}^k \int_{x_{i-1/2}}^{p_i^k} (2x - x_i) F(x_k - x, x) dx}.$$

Now, F is continuous on $[0, R] \times [0, R]$. Therefore, using mean value theorem, there exists $\xi_i, \eta_i \in (x_{i-1/2}, p_i^k)$ for $i = 1, 2, \dots, I$, such that

$$\sum_{i=1}^k \int_{x_{i-1/2}}^{p_i^k} (x_i - x) F(x_k - x, x) dx \leq \frac{1}{2} \sum_{i=1}^k F(x_k - \xi_i, \xi_i) (p_i^k - x_{i-1/2}) (x_{i+1/2} - p_i^k)$$

and

$$\sum_{i=1}^k \int_{x_{i-1/2}}^{p_i^k} (2x - x_i) F(x_k - x, x) dx \geq \sum_{i=1}^k F(x_k - \eta_i, \eta_i) (p_i^k - x_{i-1/2}) (p_i^k + x_{i-1/2} - x_i).$$

Furthermore,

$$p_i^k - x_{i-1/2} = \begin{cases} \Delta x_i, & \text{when } i \neq k, \\ \frac{1}{2} \Delta x_k, & \text{when } i = k, \end{cases} \quad x_{i+1/2} - p_i^k = \begin{cases} 0, & \text{when } i \neq k, \\ \frac{1}{2} \Delta x_k, & \text{when } i = k, \end{cases}$$

and

$$p_i^k + x_{i-1/2} - x_i = \begin{cases} x_i, & \text{when } i \neq k, \\ x_{k-1/2}, & \text{when } i = k. \end{cases}$$

Therefore, using the natural convention that $\Delta x_i \leq \Delta x_k$ whenever $i \leq k$ and condition (2.2), we get

$$\omega_k^b \leq 1 + \frac{(1/2)(\Delta x_k)^2 \sum_{i=1}^k F(x_k - \xi_i, \xi_i)}{2(\Delta x_1)^2 \sum_{i=1}^k F(x_k - \eta_i, \eta_i)} \leq 1 + \mathcal{K} + C \frac{(\Delta x)^2}{4(\delta x)^2} \leq 1 + \mathcal{K} + C\mathcal{K}^2,$$

where C is a constant independent of k and i . Next we consider the weight ω_k^d (2.7). Using relation (2.8), and the fact that $x_i \leq x_k$ for all $i = 1, 2, \dots, k$, we get

$$\omega_k^d = \frac{\omega_k^b \sum_{i=1}^k x_i \int_{x_{i-1/2}}^{p_i^k} F(x_k - x, x) dx}{\int_0^{x_k} x F(x_k - x, x) dx} = \frac{2\omega_k^b \sum_{i=1}^k x_i \int_{x_{i-1/2}}^{p_i^k} F(x_k - x, x) dx}{x_k \int_0^{x_k} F(x_k - x, x) dx} \leq 2\omega_k^b.$$

Therefore,

$$T_2 \leq \sum_{k=2}^I \omega_k^d \int_0^{x_k} F(x_k - x, x) dx |N_k - \hat{N}_k| \leq 2 \sum_{k=2}^I \omega_k^b \int_0^{x_k} F(x_k - x, x) dx |N_k - \hat{N}_k| = T_1.$$

Now, using the above relations of T_1 and T_2 and the continuity of $F(x, y)$ over $[0, R] \times [0, R]$, we can write

$$\begin{aligned} \|\mathbf{J}(\mathbf{N}) - \mathbf{J}(\hat{\mathbf{N}})\| &= T_1 + T_2 \leq 2 \sum_{k=1}^I \omega_k^b |N_k - \hat{N}_k| \int_0^{x_k} F(x_k - x, x) dx \\ &\leq 2 \max_{x \in [0, R]} \left[\int_0^x F(x - y, y) dy \right] \left[1 + \mathcal{K} + C\mathcal{K}^2 \right] \sum_{k=1}^I |N_k - \hat{N}_k| \\ &\leq \gamma \|\mathbf{N} - \hat{\mathbf{N}}\|, \end{aligned}$$

where

$$\gamma := 2 \max_{x \in [0, R]} \left[\int_0^x F(x - y, y) dy \right] \left[1 + \mathcal{K} + C\mathcal{K}^2 \right],$$

is a finite term independent of Δx . ■

We now state and prove the consistency result of the proposed model.

Proposition 3.2. *Suppose that $F(x, y) \in C^2([0, R] \times [0, R])$. Then, the solution of the discretization (3.3) is non-negative and consistent, with a truncation error of the order 2. Moreover, the method is convergent and the order of convergence is the same as the order of consistency.*

Proof. Here we need to prove three properties of the solution, namely non-negativity, consistency and convergence.

Non-negativity: Note that for any non-negative vector $\hat{\mathbf{N}} \in \mathbb{R}^I$ whose i th component equals to zero, relations (3.1) and (3.2) give,

$$\hat{B}_i(\hat{\mathbf{N}}) \geq 0 \quad \text{and} \quad \hat{D}_i(\hat{\mathbf{N}}) = 0.$$

Therefore, $\hat{J}_i(\hat{\mathbf{N}}) [= \hat{B}_i(\hat{\mathbf{N}}) - \hat{D}_i(\hat{\mathbf{N}})] \geq 0$. This observation is true for any $i = 1, \dots, I$. Hence, the non-negativity of the solution is obtained ([50], Theorem 3.1).

Consistency: The spatial truncation error is given by

$$\sigma_i(t) = \frac{dN_i(t)}{dt} - \hat{J}_i(N_i(t)) = (B_i - \hat{B}_i(\mathbf{N})) - (D_i - \hat{D}_i(\mathbf{N})).$$

Let us consider $B_i - \hat{B}_i(\mathbf{N})$ first. Recalling relations (2.3) and (3.1), we obtain

$$B_i - \hat{B}_i(\mathbf{N}) = 2 \sum_{k=i}^I (1 - \omega_k^b) N_k \int_{x_{i-1/2}}^{p_i^k} F(x_k - x, x) dx + \mathcal{O}(\Delta x^3).$$

Using definition (2.6), the term $(1 - \omega_k^b)$ is written as

$$1 - \omega_k^b = 1 - \frac{\int_0^{x_k} x F(x_k - x, x) dx}{\sum_{j=1}^k \int_{x_{j-1/2}}^{p_j^k} (2x - x_j) F(x_k - x, x) dx} = \frac{\sum_{j=1}^k \int_{x_{j-1/2}}^{p_j^k} (x - x_j) F(x_k - x, x) dx}{\sum_{j=1}^k \int_{x_{j-1/2}}^{p_j^k} (2x - x_j) F(x_k - x, x) dx}.$$

In the right-hand side of the above relation, we apply quadrature formulae and the property $F(0, x) = F(x, 0) = 0$ together with relation (2.2), to obtain

$$(1 - \omega_k^b) \int_{x_{i-1/2}}^{p_i^k} F(x_k - x, x) dx = \mathcal{O}(\Delta x^2).$$

Furthermore, applying mean value theorem, we can easily obtain

$$B_i - \hat{B}_i(\mathbf{N}) = \mathcal{O}(\Delta x^3). \tag{3.5}$$

Next we consider $D_i - \hat{D}_i(\mathbf{N})$. Recalling relations (2.4) and (3.2), we obtain

$$D_i - \hat{D}_i(\mathbf{N}) = (1 - \omega_i^d) N_i \int_0^{x_i} F(x_i - x, x) dx + \mathcal{O}(\Delta x^3).$$

In this regard, the term $1 - \omega_i^d$ is written as

$$\begin{aligned} 1 - \omega_i^d &= 1 - \frac{\omega_i^b \sum_{j=1}^i x_j \int_{x_{j-1/2}}^{p_j^i} F(x_i - x, x) dx}{\int_0^{x_i} x F(x_i - x, x) dx} = 1 - \frac{\sum_{j=1}^i x_j \int_{x_{j-1/2}}^{p_j^i} F(x_i - x, x) dx}{\sum_{j=1}^i \int_{x_{j-1/2}}^{p_j^i} (2x - x_j) F(x_i - x, x) dx} \\ &= \frac{2 \sum_{j=1}^i \int_{x_{j-1/2}}^{p_j^i} (x - x_j) F(x_i - x, x) dx}{\sum_{j=1}^i \int_{x_{j-1/2}}^{p_j^i} (2x - x_j) F(x_i - x, x) dx}. \end{aligned}$$

Now, proceeding similar to the previous case, we obtain

$$(1 - \omega_i^d) \int_0^{x_i} F(x_i - x, x) dx = \mathcal{O}(\Delta x^2),$$

which implies

$$D_i - \hat{D}_i(\mathbf{N}) = \mathcal{O}(\Delta x^3). \quad (3.6)$$

Hence, combining the two relations (3.5) and (3.6), we obtain

$$\sigma_i(t) = \mathcal{O}(\Delta x^3), \quad \text{and hence } \|\sigma(t)\| = \mathcal{O}(\Delta x^2).$$

Convergence: The above result establishes second-order consistency of the scheme (2.5). Moreover, proposition 3.1 ensures that (2.5) satisfies Lipschitz condition. Hence, recalling theorem 3.2 from [50], we obtain that the proposed one-dimensional scheme (2.5) is convergent of order 2, and this order is independent of the meshes. ■

Note: The convergence analysis of the two-dimensional scheme (2.12) can also be performed in a similar approach.

4. Numerical results

In this section, we validate the efficiency of our proposed scheme by considering several test problems. Since, the proposed scheme involves suitably chosen weight functions, so for future reference we call it *weighted finite volume scheme* (WFV scheme). The standard finite volume scheme proposed by Bourgade & Filbet [26] (BF2008) is considered to compare both the one- and two-dimensional WFV scheme. However, the two-dimensional formulation of BF2008 model is not available in the literature. Therefore, the extension of BF2008 for fragmentation events involving two particle properties is presented in appendix A.

Here, we compute the WFV scheme and BF2008 over different test problems. The assessment of the WFV scheme is done by observing its efficiency to estimate the zeroth and first moments along with the particle number density against their exact values. The dimensionless values of all the concerned quantities have been considered during the computation. In order to make the particle number density and its moments dimensionless, normalization of those properties is done by dividing their values obtained at different times by their initial values. In addition, we evaluate the *numerical order of convergence* (NOC) for the one-dimensional model. All the computations are carried up to the end time $T = 10$ in a standard computer with i3 (2.2 GHz r.p.m.) processor and 3GB RAM. The adaptive time step ODE45 solver in MATLAB is used to solve the discrete system of equations.

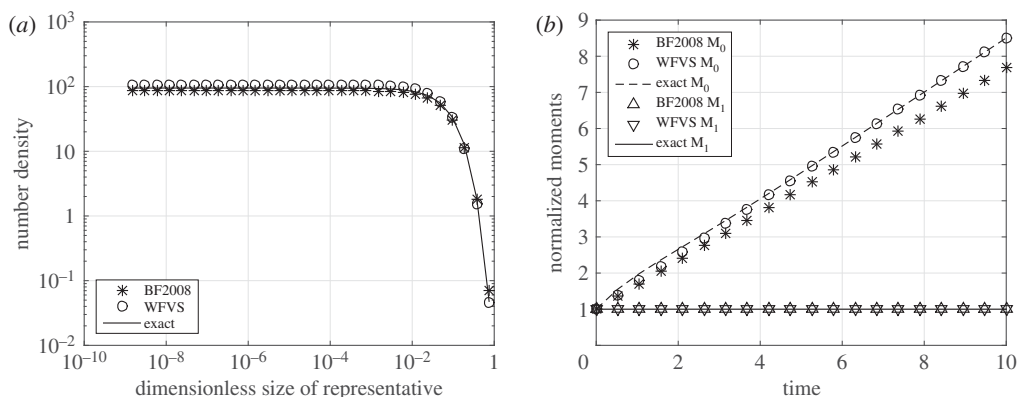


Figure 1. Exact and numerical values of the particle number density and the normalized moments (test case 1). (a) Number density and (b) moments.

(a) Examples in one dimension

Here, we consider three test problems. The exact solutions of the first two test problems are collected from [23]. The third problem is more complicated and it does not possess exact solution in closed form. All the problems are considered with mono-dispersed initial data

$$f(x, 0) = \delta(x - l) = \begin{cases} 0, & \text{when } 0 \leq x < l, \\ 1, & \text{when } x = l. \end{cases}$$

in order to minimize the accumulated error. Here, l denotes the last grid point. The computational domain is chosen to be $\mathcal{D} := [10^{-9}, 1]$.

(i) Test case 1

We consider a problem having size-independent constant fragmentation rate, $F(x, y) = 1$ for all x, y . For graphical representation, the domain \mathcal{D} is divided into 30 non-uniform meshes. The exact solution of this problem is

$$n(x, t) = \exp(-lt)\delta(x - l) + [2t + t^2(l - x)]\exp(-xt) \quad \text{when } x \leq l.$$

Figure 1 represents the comparison of numerical values of different quantities against their exact values. The number density functions are compared in figure 1a and the first and the zeroth moments given in figure 1b. From figure 1a, it is observed that both WFV scheme and BF2008 give a good estimation of the number density function, whereas the efficiency of WFV scheme over BF2008 lies in predicting the zeroth moment with high accuracy and is clearly depicted in figure 1b. Additionally, the CPU time taken for a complete run over 30 grid points as shown in figure 1 by WFV scheme is 4 s and that of BF2008 scheme is 13 s, nearly.

In table 1, we compute the the relative error and NOC of the WFV scheme over the uniform and non-uniform (geometric) meshes. NOC is calculated as follows:

$$\text{NOC} = \frac{\ln[E_I/E_{2I}]}{\ln(2)}. \quad (4.1)$$

where I is the number of pivots and $E_I = \sum_{i=1}^I |N_i^{\text{ana}} - \hat{N}_i|$ is the discrete L^1 error. To maintain a parity with the graphical results, we start the computation of NOC with 30 initial grid points. The computation is run for five times and in each run the number of grid points is doubled. Therefore, in table 1 we get five observations of the relative error and the NOC for the WFV scheme. It is obtained that the convergence rate of the WFV scheme is approximately 2 over both the meshes.

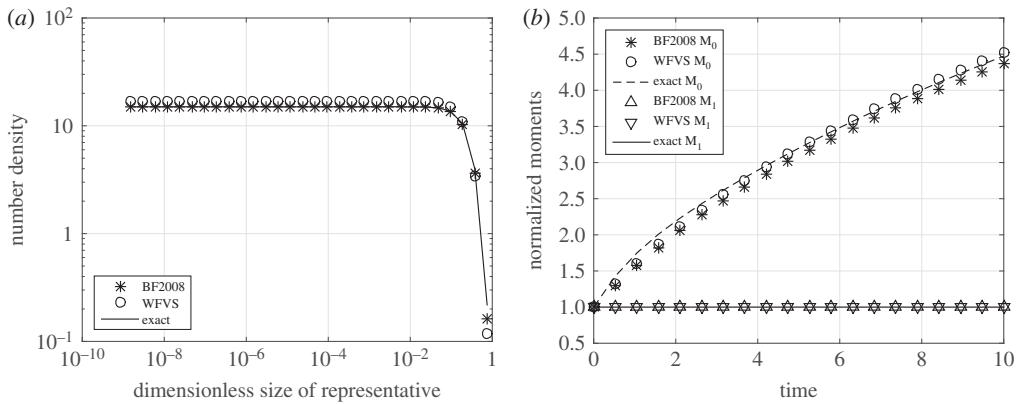


Figure 2. Exact and numerical values of the particle number density and the normalized moments (test case 2). (a) Number density and (b) moments.

Table 1. NOC of the WFV scheme for test case 1.

grids	uniform mesh		non-uniform mesh	
	relative error	NOC	relative error	NOC
30	0.0188	—	0.0573	—
60	0.0051	1.8774	0.0146	1.8199
120	0.0013	1.9409	0.0037	1.8897
240	0.0003	1.9707	0.0009	1.9487
480	0.0001	1.9833	0.0002	1.9686

However, the calculation of CPU usage time while calculating the NOC is of little interest in the literature.

(ii) Test case 2

We now consider a size-dependent fragmentation kernel satisfying $F(x, y) = x + y$ for all x, y . Like before, \mathcal{D} is divided into 30 non-uniform meshes. The exact solution of this problem is

$$n(x, t) = \exp(-tx^2)[\delta(x - l) + 2t\theta(l - x)] \quad \text{where } \theta(l - x) := \begin{cases} 1, & \text{when } x < l, \\ 0, & \text{when } x \geq l. \end{cases}$$

From figure 2, we see that both the schemes produce good estimation of the number density and conserve the first moment. However, BF2008 scheme under-predicts the zeroth moment (figure 2b) which, on the other hand, is well estimated by the WFV scheme. Like before, CPU times taken by WFV scheme and BF2008 scheme are 6 s and 19 s, respectively to solve the problem over 30 grid points.

Similar to the test case 1, we compute table 2, and it is observed that the WFV scheme shows a second-order rate of convergence over both the uniform and geometric meshes.

(iii) Test case 3

Let us consider two problems with the following size-dependent fragmentation kernels:

$$F_1(x, y) = 6 \frac{xy}{(x + y)^2} \quad \text{and} \quad F_2(x, y) = 30 \frac{x^2y^2}{(x + y)^4}.$$

Even though the exact solutions are not available, we can calculate the moments exactly.

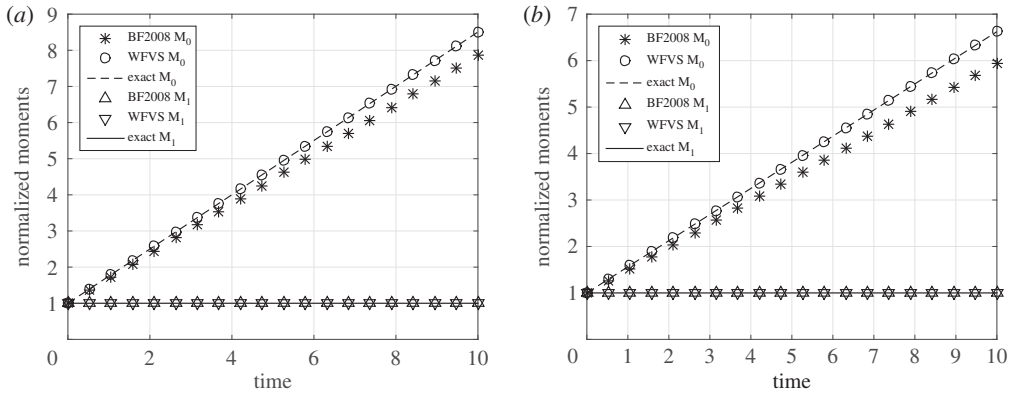


Figure 3. Exact and numerical values of the normalized moments (test case 3). (a) Kernel F_1 and (b) kernel F_2 .

Table 2. NOC of the WFV scheme for test case 2.

grids	uniform mesh		non-uniform mesh	
	relative error	NOC	relative error	NOC
30	0.0195	—	0.0788	—
60	0.0058	1.9310	0.0204	1.7782
120	0.0017	1.9613	0.0052	1.8823
240	0.0003	1.9687	0.0013	1.9450
480	0.0001	1.9451	0.0003	1.9655

Table 3. NOC of the WFV scheme in test case 3 with kernels F_1 and F_2 .

grids	kernel F_1				kernel F_2			
	uniform mesh		non-uniform mesh		uniform mesh		non-uniform mesh	
	relative error	NOC	relative error	NOC	relative error	NOC	relative error	NOC
30	—	—	—	—	—	—	—	—
60	0.1803	—	0.0340	—	1.2720	—	1.2694	—
120	0.0512	1.8176	0.0103	1.7182	0.2678	2.2476	0.2737	2.2136
240	0.0136	1.9081	0.0026	1.9670	0.2678	2.2476	0.0632	2.1156
480	0.0035	1.9542	0.0007	1.9905	0.0153	2.0510	0.0151	2.0614

Figure 3a,b represents the normalized moments corresponding to the problems with the kernels, $F_1(x, y)$ and $F_2(x, y)$. The CPU time taken by WFV scheme is approximately 5 s for both the problems, whereas CPU time for BF2008 scheme for F_1 is 17 s and that of F_2 is 19 s over 30 grid points. Furthermore, the relative error and NOC of the WFV scheme for both the problems are calculated using the following relation:

$$NOC = \frac{\ln[\|\hat{N}_I - \hat{N}_{2I}\|/\|\hat{N}_{2I} - \hat{N}_{4I}\|]}{\ln(2)}, \tag{4.2}$$

where I is the number of grid points, \hat{N} is the numerical value of the density function [51] (table 3).

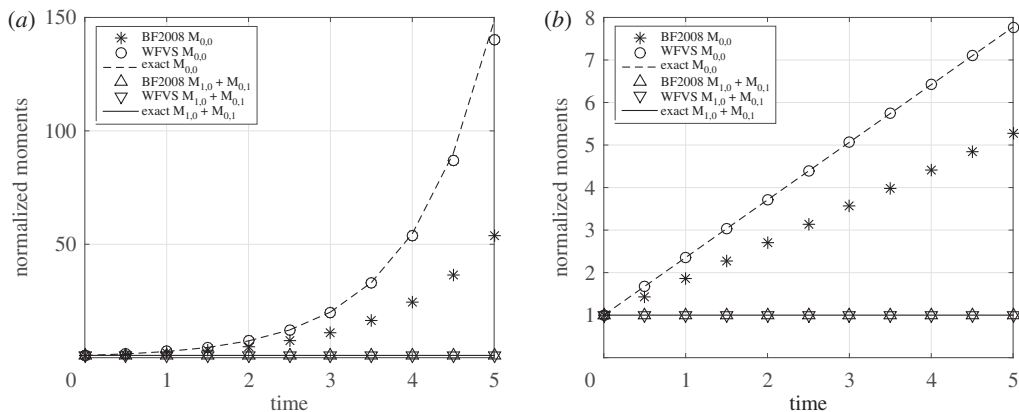


Figure 4. Exact and numerical values of the normalized moments (test case 4). (a) Kernel F_a and (b) Kernel F_b .

(b) Examples in two dimensions

For the two-dimensional problems, we analyse the efficiency of WFV scheme both qualitatively and quantitatively. The qualitative comparison includes a flat graphical representation of the zeroth- and first-order moment functions, as followed in the literature by Kumar *et al.* [47,49]. In flat representation, the moments on each pivot are plotted against the index. To obtain a systematic plot, the moments are sorted in decreasing order of their exact values. On the other hand, weighted errors are evaluated to determine the accuracy of the moment functions quantitatively. A general measure of the weighted error for two-dimensional problems is given as [47]

$$\mu_{ij} := \max_t \left| \frac{M_{ij}^{ana}(t) - M_{ij}^{num}(t)}{M_{ij}^{ana}(t)} \right|.$$

(i) Test case 4

Here, we consider two fragmentation kernels given by

$$F_a(x_1, y_1|x, y) := \frac{2}{(x_1 + x)(y_1 + y)} \quad \text{and} \quad F_b(x_1, y_1|x, y) := \frac{2(x_1 + x + y_1 + y)}{(x_1 + x)(y_1 + y)}.$$

In both the cases, the problems are supported by the mono-dispersed initial data $f(x, y, 0) = \delta(x - l_x)\delta(y - l_y)$, where l_x and l_y , respectively, correspond to the last pivots along x - and y -directions. The computational domain considered to be $[10^{-9}, 1] \times [10^{-9}, 1]$ and it is divided into 12×12 geometric grids. The exact solutions of these problems are not available in the literature. However, the moment functions can be calculated exactly for these kernels. In figure 4, we plot the zeroth and the first moments predicted by two-dimensional WFV and BF2008 schemes and compare them against the exact values. Figure 4a corresponds to the problem with kernel F_a and figure 4b corresponds to F_b . The weighted errors of different moments are given in table 4. Like the one-dimensional case, we see that WFV scheme produces highly accurate estimation of the zeroth moment. On the other hand, two-dimensional BF2008 scheme produces a quite under-predicted estimation of the zeroth moment over coarser grids. As, the sample problems do not have exact solutions, to evaluate the numerical order of convergence, one needs to use an extended version of relation (4.2). However, computation of NOC over rectangular meshes is very cumbersome and involves high CPU usage time. Moreover, the results obtained are similar to those of one-dimensional cases. Therefore, calculation of NOC for the two-dimensional sample problems is of little interest.

Table 4. Maximum error in zeroth- and first-order moments.

μ	kernel K_a		kernel K_b	
	BF2008	WFVS	BF2008	WFVS
$\mu_{0,0}$	0.8437	0.0783	0.3222	6.7955×10^{-4}
$\mu_{1,0} + \mu_{0,1}$	0.0031	2.2982×10^{-4}	8.2636×10^{-5}	1.1132×10^{-5}

In order to generate figure 4, the WFV scheme consumed 5 s and 6 s of CPU time to solve the problems with kernels K_a and K_b , respectively. On the other hand, the BF2008 scheme required 29 s and 33 s of CPU time for solving the similar set of problems.

5. Conclusion

In this work, we present an efficient finite volume scheme to approximate the fragmentation equations. The basic idea is to preserve total volume of the particles, and, to estimate total particle number present in the system with good accuracy. This is done by introducing suitable weight functions in both the discrete birth and death terms. The development of the one-dimensional model is completed by studying stability and consistency of the scheme. It is observed that the one-dimensional scheme is second-order convergent and the rate being independent of the meshes. Furthermore, we extend the proposed model for solving the problems in two dimensions. It is observed that the literature has no evidence on multi-dimensional finite volume scheme for fragmentation problems. So, to validate the efficiency of our proposed two-dimensional model, we need some reference model in two variables. Therefore, we introduce the two-dimensional extension of the standard finite volume model proposed by [26]. The efficiency of our proposed model is validated over several test problems.

Ethics. This work involves mathematical modelling and computer simulations only.

Data accessibility. This work does not have any experimental data.

Authors' contributions. J.S. proposed and solved the problem and J.K. and S.H. provided technical details and physical interpretation of the proposed problem.

Competing interests. We do not have any competing interests.

Funding. This research received no specific grant from any funding agency, commercial or not-for-profit sectors.

Appendix A. Two-dimensional extension of BF2008 model

To compare the efficiency of two-dimensional WFV scheme, we introduce the two-dimensional extension of BF2008. For a smooth reading, we first recall one-dimensional BF2008.

Referring to [26], the semi-discrete BF2008 scheme is written as

$$\frac{d(x_i N_i)}{dt} = \mathcal{V}_{i+1/2} - \mathcal{V}_{i-1/2}, \quad (\text{A } 1)$$

with the initial data

$$N_i^{\text{in}} = n_i^{\text{in}} \Delta x_i = \int_{\Lambda_i} n(x, 0) dx.$$

The function $\mathcal{V}_{i+1/2}$ denotes the volume-flux at the right boundary of Λ_i and is given by

$$\mathcal{V}_{i+1/2} := \sum_{j=1}^i \sum_{k=i+1}^I x_j F_{j,k} N_k \Delta x_j,$$

under the consideration that $\mathcal{V}_{1/2} = \mathcal{V}_{I+1/2} = 0$. Here, $F_{j,k}$ represents the breakage of particles of volume k into smaller pieces of volumes j and $(k-j)$.

The continuous two-dimensional volume conservative pure breakage equation is written as

$$(x+y) \frac{\partial n(x,y,t)}{\partial t} = \frac{\partial \mathcal{F}(x,y,t)}{\partial x} + \frac{\partial \mathcal{G}(x,y,t)}{\partial y} - \frac{\partial^2 \mathcal{H}(x,y,t)}{\partial x \partial y}, \quad (\text{A } 2)$$

where

$$\mathcal{F}(x,y,t) := \int_0^x \int_{x-u}^\infty \int_0^\infty (u+y)F(u,y|v,w)n(u+v,y+w,t) \, dw \, dv \, du,$$

$$\mathcal{G}(x,y,t) := \int_0^y \int_{y-u}^\infty \int_0^\infty (u+x)F(x,u|w,v)n(x+w,u+v,t) \, dw \, dv \, du,$$

and
$$\mathcal{H}(x,y,t) := \int_0^x \int_0^y \int_{x-u}^\infty \int_{y-v}^\infty (u+v)F(u,v|w,z)n(u+w,v+z,t) \, dz \, dw \, dv \, du.$$

It is to be noted that relations (2.9) and (A 2) are mathematically equivalent. (Similar calculations have been performed in [45] for pure aggregation problems.)

Proceeding similarly as done in §2b, we get the following semi-discrete model,

$$\begin{aligned} \frac{dN_{ij}}{dt}(x_i+y_j) &= [\tilde{\mathcal{F}}_{i+1/2,j} - \tilde{\mathcal{F}}_{i-1/2,j}]\Delta y_j + [\tilde{\mathcal{G}}_{i,j+1/2} - \tilde{\mathcal{G}}_{i,j-1/2}]\Delta x_i \\ &\quad - [\tilde{\mathcal{H}}_{i+1/2,j+1/2} - \tilde{\mathcal{H}}_{i+1/2,j-1/2} - \tilde{\mathcal{H}}_{i-1/2,j+1/2} + \tilde{\mathcal{H}}_{i-1/2,j-1/2}], \end{aligned} \quad (\text{A } 3)$$

along with the initial data

$$N_{ij}^{\text{in}} = \int_{C_{ij}} n(x,y,0) \, dx \, dy.$$

Derivation of the fluxes $\tilde{\mathcal{F}}$, $\tilde{\mathcal{G}}$ and $\tilde{\mathcal{H}}$ are obtained as follows.

The conservative truncation of $\mathcal{F}(x,y,t)$ is written as

$$\tilde{\mathcal{F}}(x,y,t) = \int_0^x \int_{x-u}^{R_x-u} \int_0^{R_y-w} (u+y)F(u,y|v,w)n(u+v,y+w,t) \, dw \, dv \, du.$$

Therefore, flux at the cell interface is given by

$$\tilde{\mathcal{F}}(x_{i+1/2}, y_j, t) = \int_0^{x_{i+1/2}} \int_{x_{i+1/2}}^{R_x} \int_{y_j}^{R_y} (u+y_j)F(u,y_j|v-u, w-y_j)n(v,w,t) \, dw \, dv \, du.$$

Applying quadrature formulae, we obtain

$$\tilde{\mathcal{F}}_{i+1/2,j}(t) := \sum_{i_1=1}^i \sum_{k_1=i+1}^I \sum_{j_1=j+1}^J (x_{i_1} + y_{j_1})F_{i_1,j_1|k_1,j_1} N_{k_1,j_1} \Delta x_{i_1}.$$

Similarly, we can write

$$\tilde{\mathcal{G}}_{i,j+1/2}(t) := \sum_{j_1=1}^j \sum_{l_1=j+1}^J \sum_{i_1=i+1}^I (x_{i_1} + y_{j_1})F_{i_1,j_1|i_1,l_1} N_{i_1,l_1} \Delta y_{j_1}$$

and

$$\tilde{\mathcal{H}}_{i+1/2,j+1/2}(t) := \sum_{i_1=1}^i \sum_{j_1=1}^j \sum_{k_1=i+1}^I \sum_{l_1=j+1}^J (x_{i_1} + y_{j_1})F_{i_1,j_1|k_1,l_1} N_{k_1,l_1} \Delta y_{j_1} \Delta x_{i_1}.$$

Now, substituting the terms $\tilde{\mathcal{F}}$, $\tilde{\mathcal{G}}$ and $\tilde{\mathcal{H}}$ in the right-hand side of the above semi-discrete formulation and performing some mathematical computations, the relation (A 3) can be written as

$$\begin{aligned} \frac{dN_{ij}}{dt}(x_i + y_j) = & \sum_{k_1=i}^I \sum_{l_1=j}^J (x_i + y_j) N_{k_1, l_1} F_{i, j | k_1, l_1} \Delta x_i \Delta y_j \\ & - \sum_{i_1=1}^i \sum_{j_1=1}^j (x_{i_1} + y_{j_1}) N_{i, j} F_{i_1, j_1 | i, j} \Delta x_{i_1} \Delta y_{j_1}. \end{aligned} \quad (\text{A } 4)$$

Thus, relation (A 4) represents the two-dimensional extension of [26] model in a simplified form.

References

1. Litster J, Ennis B. 2004 Breakage and attrition. In *The science and engineering of granulation processes*, ch. 5, pp. 121–142. Berlin, Germany: Springer.
2. Gokhale Y, Kumar R, Kumar J, Hintz W, Warnecke G, Tomas J. 2009 Disintegration process of surface stabilized sol-gel TiO₂ nanoparticles by population balances. *Chem. Eng. Sci.* **64**, 5302–5307. (doi:10.1016/j.ces.2009.09.015)
3. Ramachandran R, Immanuel C, Stepanek F, Litster J, Doyle F. 2009 A mechanistic model for breakage in population balances of granulation: Theoretical kernel development and experimental validation. *Chem. Eng. Res. Design* **87**, 598–614. (doi:10.1016/j.cherd.2008.11.007)
4. Quarch K, Durand E, Kind M. 2010 Inorganic precipitated silica gel. Part 2: fragmentation by mechanical energy. *Chem. Eng. Technol.* **33**, 1208–1212. (doi:10.1002/ceat.201000081)
5. Kind M. 1999 Product engineering. *Chem. Eng. Process.: Process Intensification* **38**, 405–410. (doi:10.1016/S0255-2701(99)00038-0)
6. Nijdam J, Ibach A, Eichhorn K, Kind M. 2007 An X-ray diffraction analysis of crystallised whey and whey-permeate powders. *Carbohydr. Res.* **342**, 2354–2364. (doi:10.1016/j.carres.2007.08.001)
7. Maas S, Schaldach G, Walzel P, Urbanetz N. 2010 Tailoring dry powder inhaler performance by modifying carrier surface topography by spray drying. *Atomization Sprays* **20**, 763–774. (doi:10.1615/AtomizSpr.v20.i9.20)
8. Albion K, Briens L, Briens C, Berruti F. 2006 Detection of the breakage of pharmaceutical tablets in pneumatic transport. *Int. J. Pharm.* **322**, 119–129. (doi:10.1016/j.ijpharm.2006.05.039)
9. Parveen F, Josset S, Briens C, Berruti F. 2012 Effect of size and density on agglomerate breakage in a fluidized bed. *Powder Technol.* **231**, 102–111. (doi:10.1016/j.powtec.2012.07.055)
10. Cornehl B, Overbeck A, Schwab A, Büser J, Kwade A, Nirschl H. 2014 Breakage of lysozyme crystals due to compressive stresses during cake filtration. *Chem. Eng. Sci.* **111**, 324–334. (doi:10.1016/j.ces.2014.02.016)
11. Kwade A, Schwedes J. 2002 Breaking characteristics of different materials and their effect on stress intensity and stress number in stirred media mills. *Powder Technol.* **122**, 109–121. (doi:10.1016/S0032-5910(01)00406-5)
12. Fuerstenau D, De A, Kapur P. 2004 Linear and nonlinear particle breakage processes in comminution systems. *Int. J. Mineral Process.* **74**, S317–S327. (doi:10.1016/j.minpro.2004.07.005)
13. Smith R, Liu L, Litster J. 2010 Breakage of drop nucleated granules in a breakage only high shear mixer. *Chem. Eng. Sci.* **65**, 5651–5657. (doi:10.1016/j.ces.2010.06.037)
14. Wengeler R, Teleki A, Vetter M, Pratsinis S, Nirschl H. 2006 High-pressure liquid dispersion and fragmentation of flame-made silica agglomerates. *Langmuir* **22**, 4928–4935. (doi:10.1021/la053283n)
15. Fowler A, Scheu B, Lee W, McGuinness M. 2010 A theoretical model of the explosive fragmentation of vesicular magma. *Proc. R. Soc. A* **466**, 731–752. (doi:10.1098/rspa.2009.0382)
16. Hauk T, Bonaccorso E, Roisman I, Tropea C. 2015 Ice crystal impact onto a dry solid wall. particle fragmentation. *Proc. R. Soc. A* **471**, 20150399. (doi:10.1098/rspa.2015.0399)
17. Fowler A, Scheu B. 2016 A theoretical explanation of grain size distributions in explosive rock fragmentation. *Proc. R. Soc. A* **472**, 20150843. (doi:10.1098/rspa.2015.0843)
18. Stewart I. 1990 On the coagulation-fragmentation equation. *Z. Angew. Math. Phys.* **41**, 917–924. (doi:10.1007/BF00945844)

19. Ziff R. 1991 New solutions to the fragmentation equation. *J. Phys. A: Math. Gen.* **24**, 2821–2828. (doi:10.1088/0305-4470/24/12/020)
20. Kumar R, Kumar J. 2013 Numerical simulation and convergence analysis of a finite volume scheme for solving general breakage population balance equations. *Appl. Math. Comput.* **219**, 5140–5151. (doi:10.1016/j.amc.2012.10.098)
21. Saha J, Kumar J. 2015 The singular coagulation equation with multiple fragmentation. *Z. Angew. Math. Phys.* **66**, 919–941. (doi:10.1007/s00033-014-0452-3)
22. Vledouts A, Vandenberghe N, Villermaux E. 2015 Fragmentation as an aggregation process. *Proc. R. Soc. A* **471**, 20150678. (doi:10.1098/rspa.2015.0678)
23. Ziff R, McGrady E. 1985 The kinetics of cluster fragmentation and depolymerisation. *J. Phys. A: Math. Gen.* **18**, 3027–3037. (doi:10.1088/0305-4470/18/15/026)
24. Ramkrishna D. 2000 *Population balances: theory and applications to particulate systems in engineering*. New York, NY: Academic press.
25. Filbet F, Laurençot P. 2004 Numerical simulation of the Smoluchowski coagulation equation. *SIAM. J. Sci. Comput.* **25**, 2004–2028. (doi:10.1137/S1064827503429132)
26. Bourgade J, Filbet F. 2008 Convergence of a finite volume scheme for coagulation-fragmentation equations. *Math. Comput.* **77**, 851–882. (doi:10.1090/S0025-5718-07-02054-6)
27. Oddershede L, Dimon P, Bohr J. 1993 Self-organized criticality in fragmenting. *Phys. Rev. Lett.* **71**, 3107. (doi:10.1103/PhysRevLett.71.3107)
28. Ishii T, Matsushita M. 1992 Fragmentation of long thin glass rods. *J. Phys. Soc. Japan* **61**, 3474–3477. (doi:10.1143/JPSJ.61.3474)
29. Ernst M, Szamel G. 1993 Fragmentation kinetics. *J. Phys. A: Math. Gen.* **26**, 6085. (doi:10.1088/0305-4470/26/22/011)
30. Singh P, Hassan M. 1996 Kinetics of multidimensional fragmentation. *Phys. Rev. E* **53**, 3134. (doi:10.1103/PhysRevE.53.3134)
31. Ben-Naim E, Krapivsky P. 1997 Multiscaling in fragmentation. *Phys. D: Nonlinear Phenom.* **107**, 156–160. (doi:10.1016/S0167-2789(97)00080-8)
32. Boyer D, Tarjus G, Viot P. 1997 Exact solution and multifractal analysis of a multivariable fragmentation model. *J. Phys. I* **7**, 13–38. (doi:10.1051/jp1:1997125)
33. Kumar S, Ramkrishna D. 1996 On the solution of population balance equations by discretization—I. A fixed pivot technique. *Chem. Eng. Sci.* **51**, 1311–1332. (doi:10.1016/0009-2509(96)88489-2)
34. Kumar S, Ramkrishna D. 1996 On the solution of population balance equations by discretization—II. A moving pivot technique. *Chem. Eng. Sci.* **51**, 1333–1342. (doi:10.1016/0009-2509(95)00355-X)
35. Kumar J, Peglow M, Warnecke G, Heinrich S, Mörl L. 2006 Improved accuracy and convergence of discretized population balance for aggregation: the cell average technique. *Chem. Eng. Sci.* **61**, 3327–3342. (doi:10.1016/j.ces.2005.12.014)
36. Kostoglou M, Karabelas A. 2002 An assessment of low-order methods for solving the breakage equation. *Powder. Technol.* **127**, 116–127. (doi:10.1016/S0032-5910(02)00110-9)
37. Kostoglou M, Karabelas A. 2004 Optimal low order methods of moments for solving the fragmentation equation. *Powder. Technol.* **143**, 280–290. (doi:10.1016/j.powtec.2004.04.020)
38. Nicmanis M, Hounslow M. 1998 Finite-element methods for steady-state population balance equations. *AIChE J.* **44**, 2258–2272. (doi:10.1002/aic.690441015)
39. Ganesan S. 2012 An operator-splitting Galerkin/SUPG finite element method for population balance equations: stability and convergence. *ESAIM: Math. Model. Numer. Anal.* **46**, 1447–1465. (doi:10.1051/m2an/2012012)
40. Ganesan S, Tobiska L. 2012 An operator-splitting finite element method for the efficient parallel solution of multidimensional population balance systems. *Chem. Eng. Sci.* **69**, 59–68. (doi:10.1016/j.ces.2011.09.031)
41. Qamar S, Warnecke G. 2007 Numerical solution of population balance equations for nucleation, growth and aggregation processes. *Comput. Chem. Eng.* **31**, 1576–1589. (doi:10.1016/j.compchemeng.2007.01.006)
42. Forestier-Coste L, Mancini S. 2012 A finite volume preserving scheme on nonuniform meshes and for multidimensional coalescence. *SIAM. J. Sci. Comput.* **34**, B840–B860. (doi:10.1137/110847998)
43. Kumar R, Kumar J, Warnecke G. 2013 Moment preserving finite volume schemes for solving population balance equations incorporating aggregation, breakage, growth and source terms. *Math. Models Methods Appl. Sci.* **23**, 1235–1273. (doi:10.1142/S0218202513500085)

44. Kumar J, Saha J, Tsotsas E. 2015 Development and convergence analysis of a finite volume scheme for solving breakage equation. *SIAM. J. Numer. Anal.* **53**, 1672–1689. (doi:10.1137/140980247)
45. Qamar S, Warnecke G. 2007 Solving population balance equations for two-component aggregation by a finite volume scheme. *Chem. Eng. Sci.* **62**, 679–693. (doi:10.1016/j.ces.2006.10.001)
46. Singh M, Kumar J, Bück A, Tsotsas E. 2015 A volume-consistent discrete formulation of aggregation population balance equations. *Math. Methods Appl. Sci.* **39**, 2275–2286. (doi:10.1002/mma.3638)
47. Singh M, Kumar J, Bück A, Tsotsas E. 2016 An improved and efficient finite volume scheme for bivariate aggregation population balance equation. *J. Comput. Appl. Math.* **308**, 83–97. (doi:10.1016/j.cam.2016.04.037)
48. Kumar J, Kaur G, Tsotsas E. 2016 An accurate and efficient discrete formulation of aggregation population balance equation. *Kinet. Relat. Models* **9**, 373–391. (doi:10.3934/krm.2016.9.373)
49. Kaur G, Kumar J, Heinrich S. 2017 A weighted finite volume scheme for multivariate aggregation population balance equation. *Comput. Chem. Eng.* **101**, 1–10. (doi:10.1016/j.compchemeng.2017.02.011)
50. Saha J, Kumar J, Heinrich S. 2017 A volume-consistent discrete formulation of particle breakage equation. *Comput. Chem. Eng.* **97**, 147–160. (doi:10.1016/j.compchemeng.2016.11.013)
51. Kumar J, Warnecke G. 2008 Convergence analysis of sectional methods for solving breakage population balance equations—I: the fixed pivot technique. *Numer. Math.* **111**, 81–108. (doi:10.1007/s00211-008-0174-6)